Characterization of the DNA triplex formed by d(TGGGTGGGTGGTTGGGTGGG) and a critical R·Y sequence located in the promoter of the murine Ki-*ras* proto-oncogene

Luigi E. Xodo*

Department of Biochemistry, Biophysics and Macromolecular Chemistry, Via Giorgieri 1, University of Trieste, 34127 Trieste, Italy

Received 19 June 1995; revised version received 10 July 1995

Abstract The binding of the G-rich oligonucleotide d(TGGGTGGGTGGTTGGGTGGG) to a critical homopurine–homopyrimidine sequence located in the promoter of the murine Ki-*ras* proto-oncogene has been investigated. The duplex and the oligonucleotide form a triple helix as evidenced by band-shift electrophoresis, hydroxyapatite (HA) chromatography, UV-melting and circular dichroism (CD) experiments. Upon thermal denaturation in 50 mM Tris-acetate, pH 7.4, 50 mM NaCl, 10 mM $MgCl_2$, 0.1 mM spermine the triplex exhibits two cooperative transitions: one of these is attributed to the *triplex-to-duplex* transformation, the other to the *duplex-to-coil* transformation. The thermodynamic parameters of triplex formation have been determined by a van't Hoff analysis of the UV-melting curves which provided values of $\Delta H = 79 \pm 8$ kcal/mol, $\Delta S = 224 \pm 22$ e.u., $\Delta G_{298} = 12.2 \pm 1.2$ kcal/mol. These data are compared with those reported for the YRY triplex motif.

Key words: Ki-*ras*; Polypurine–polypyrimidine; DNA triplex; Circular dichroism; UV-melting; Thermodynamics

1. Introduction

Pyrimidine oligonucleotides directed against polypurine–polypyrimidine (R·Y) tracts of DNA can form triple helices stabilised by C^+·GC and TAT base triplets (Y·RY triplex) (see review in [1]). Such DNA structures have been studied with different methods including eletrophoresis [2–4], UV-spectroscopy [5–13] and NMR [14,15].

In addition to Y·RY triplexes, a second triple-helical motif, namely the R·RY triplex, can be obtained when a G-rich oligonucleotide is used as third strand [16–19]. G-Rich oligonucleotides bind the polypurine tracts of duplex DNA with an antiparallel orientation, forming either G·GC and T·AT triads, if the third strand is a (G,T)-oligonucleotide, or G·GC and A·TA triads, if the third strand is a (G,A)-oligonucleotide [1].

The first evidence about the formation of R·RY triplexes was obtained with mixtures of poly(G) plus poly(C) [20,21] and poly(U) plus poly(A) [22]. Thereafter, Kohwi and Kowhi-Shigematzu demonstrated that a segment of poly dG·poly(dC), if inserted in a supercoiled plasmid, adopted in the presence of Mg^{2+} an intramolecular structure stabilised by G·GC triads [23].

*Corresponding author. Fax: (39) (40) 67-6369.
E-mail: xodo@univ.trieste.it

Abbreviations: CD, circular dichroism; UV, ultraviolet absorbance; HA, hydroxyapatite; R·Y, polypurine·polypyrimidine.

Recently, several research groups have drawn the attention on G-rich oligonucleotides, since these compounds may be used as transcription repressors because of their ability to bind duplex DNA in a sequence-specific manner under physiological conditions, [16,24–26].

To date, R·R·Y triple helices have been characterised by electrophoresis, foot-printing and NMR experiments [17,18,27–29]. There are no stability data about this type of triplexes, except for a thermodynamic analysis regarding the formation of a triplex made by a 10-mer (G,A)-oligonucleotide [19]. The aim of the present communication is to report experiments characterising the triple-helical complex formed by d(TGGGTGGGTGGTTGGGTGGG) (20GT) and a RY duplex of 30 bp in length (30RY). This duplex corresponds to a critical sequence located in the promoter region of the murine Ki-*ras* proto-oncogene, which is essential for transcription activity as it is the binding site of a transcription factor [30]. To the author's knowledge, this is the first time that a thermodynamic analysis of triplex formation involving as third strand a (G,T)-oligonucleotide is reported.

2. Materials and methods

2.1. Synthesis and purification of the deoxyoligonucleotides

The deoxyoligonucleotides used in this study have been synthesised in solid phase using standard phosphoroamidite chemistry. The fully deprotected synthesis products were passed through a Mono-Q HR column (Pharmacia), eluted with a gradient of ammonium bicarbonate. Purity was checked by 20% PAGE in denaturing conditions. Buffer reagents were purchased from Sigma Chemical Co., PAGE reagents from Serva.

2.2. Gel electrophoresis

Non-denaturing 15% PAGE (29:1; acrylamide:bis-acrylamide) was carried out in 50 mM Tris-acetate (pH 7.4), 50 mM NaCl, 10 mM $MgCl_2$. Mixtures of duplex 30RY and oligonucleotide 20GT were examined in a 10 cm gel at 7 V/cm, at room temperature. After the electrophoresis the gel was stained with *stains-all* dye in water/formamide 1:1 (overnight), and photographed with a polaroid camera.

2.3. Spectroscopy

Ultraviolet (UV) absorption spectra and thermal denaturation profiles were recorded with a Cary 2200 (Varian) spectrophotometer equipped with temperature-regulated cuvette-holder. The cuvette-holder was thermostated by a circulating liquid, whose temperature was controlled by a Haake PG20 temperature programmer. The temperature of the bath was increased and decreased at a rate of 0.5°C/min. DNA concentrations were determined by UV absorbance at 260 nm using as extinction coefficients 7500, 8500, 15000 and 12500 $M^{-1} \cdot cm^{-1}$ for C, T, A and G, respectively, in the denatured state. The melting experiments were performed in 50 mM Tris-acetate (pH 7.4), 50 mM NaCl, 10 mM $MgCl_2$, 0.1 mM spermine (standard buffer).

SSDI 0014-5793(95)00829-2

2.4. Circular dichroism and hydroxyapatite (HA) chromatography

CD spectra were recorded with a Jasco J-500 A spectropolarimeter connected with a Jasco DP 500 N data processor. Spectra are presented as $\Delta\varepsilon = \varepsilon_L - \varepsilon_R$ in units of $M^{-1} \cdot cm^{-1}$. The spectra were recorded using 2 mm pathlength cuvette containing DNA at a concentration in the range from 2 to 4 μM in single strand (or duplex or triplex). Mixtures of 30RY and 20GT at different ratios were examined by HA chromatography (column: 100 mm length, 7.6 mm inner diameter; packed by Mitsui Toatsu, Japan). The DNA mixtures, prepared in standard buffer, were left at 4°C for 12 h before being fractionated with a HA column eluted with a phosphate buffer (pH 7.4) in a gradient from 0 to 500 mM in 60 min, at a flow rate of 1 ml/min.

3. Results and discussion

3.1. RY target site used in this study

A R·Y sequence located in the promoter of the murine Ki-*ras* proto-oncogene, essential for transcription activity, was chosen as a target for a G-rich triplex-forming oligonucleotide of sequence d(TGGGTGGGTGGTTGGGTGGG) (20GT). The primary structure of the critical Ki-*ras* target duplex (30RY) is illustrated in Fig. 1. The oligonucleotide 20GT was designed to bind the major groove of 30RY with an antiparallel orientation with respect to the purine strand of 30RY [17–19]. The resulting R·RY triplex should contain G·GC and T·AT base triplets in the reverse Hoogsteen configuration [17,28]. Both 20GT and 30RY were synthesised in order to study their interaction under physiological pH.

3.2. Polyacrylamide gel electrophoresis and HA chromatography

The ability of 20GT to bind the target duplex 30RY was analysed by eletrophoresis on a 15% polyacrylamide gel in 50 mM Tris-acetate, pH 7.4, 50 mM NaCl, 10 mM $MgCl_2$. Fig. 2 shows the retardation in electrophoretic mobility occurring to duplex 30RY when mixed with 20GT heated to 90°C for 5 min in order to disrupt the aggregates that this G-rich oligonucleotide forms slowly (within hours) in solution. The result clearly suggests that the mixture forms a DNA complex which can be attributed to a triplex.

Mixtures of 20GT and 30RY at various ratios were also analysed by hydroxyapatite chromotography after the samples were left at 4°C for 12 h. Under these experimental conditions, it was found that single strand 20GT was eluted with a retention time (t_R) of 3.9 min, double-strand 30RY was eluted with a t_R = 8.4 min and triple-strand DNA with a t_R = 12.8 min (not shown). This technique appeared to be valuable for a rapid detection of triplex formation by duplex and single strand DNA; however, the reproducibility proved sometimes to be problematic unless some parameters (i.e. column pre-washing,

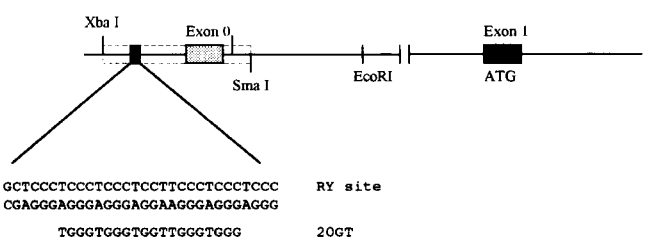

Fig. 1. Structure of the 5′ region of the mouse c-Ki-*ras* gene and sequence of the homopurine–homopyrimidine (R·Y) stretch essential for transcription activity. The R·Y sequence is a potential site for triplex-forming oligonucleotide 20GT.

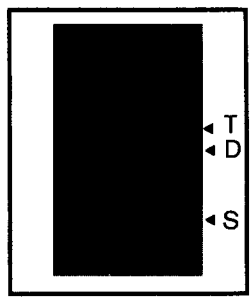

Fig. 2. 15% polyacrylamide gel electrophoresis in 50 mM Tris-HCl (pH 7.4), 50 mM NaCl, 10 mM $MgCl_2$ of duplex 30RY (lane 1), triplex-forming oligonucleotide 20GT (lane 2), mixture 20GT:30RY at 1:2 ratio (lane 3). 20GT before being added to preformed 30RY was heated at 90 for 5 min. The mixture was left at room temperature for few hours before PAGE analysis. Symbols: T = triplex; D = duplex; S = single strand.

sample volume injected, buffer quality, ...) were rigourously held constant [31].

3.3. Circular dichroism

Fig. 3 shows the CD spectra of 20GT, 30RY and of an equimolar mixture between 30RY and 20GT after each sample had been incubated for 12 h at 4°C. The fact that the spectrum of 20GT:30RY is different from the sum of individual 30RY and 20GT spectra suggests that there is an interaction between the two components of the mixture, thus forming a triple-helical complex. Interestingly, an intense and negative ellipticity at 212 nm is induced upon triplex formation, as previously observed for other triplex structures [5,6,24]. Another outstanding feature present in the 20GT:30RY spectrum is the presence of a negative ellipticity at 277 nm, which according to a study on poly(dG)·poly(dC) has been attributed to the formation of triplex helices containing G·GC triads [20,21,32,33].

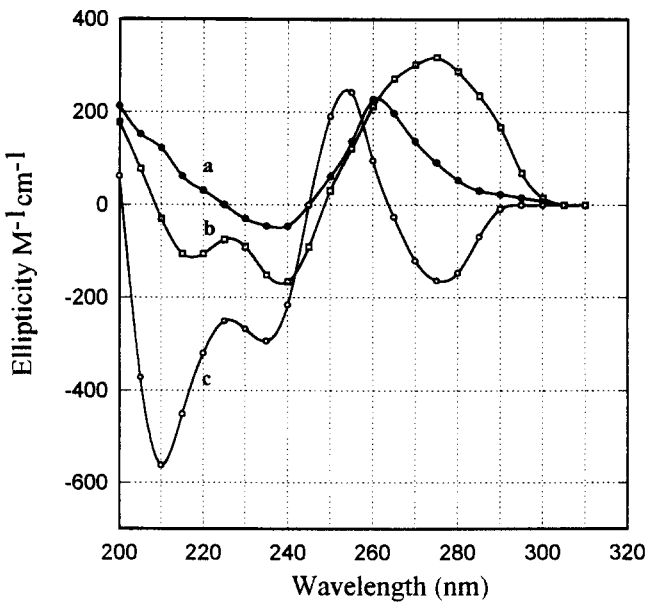

Fig. 3. Circular dichroism spectra of (a) 20GT; (b) 30RY; (c) equimolar mixture between 20GT and 30RY, after being incubated at 4°C for 12 h. Spectra were recorded using a 2 mm wavelength cuvette and the samples were at concentrations 1.7 μM in single strand (or duplex or triplex)

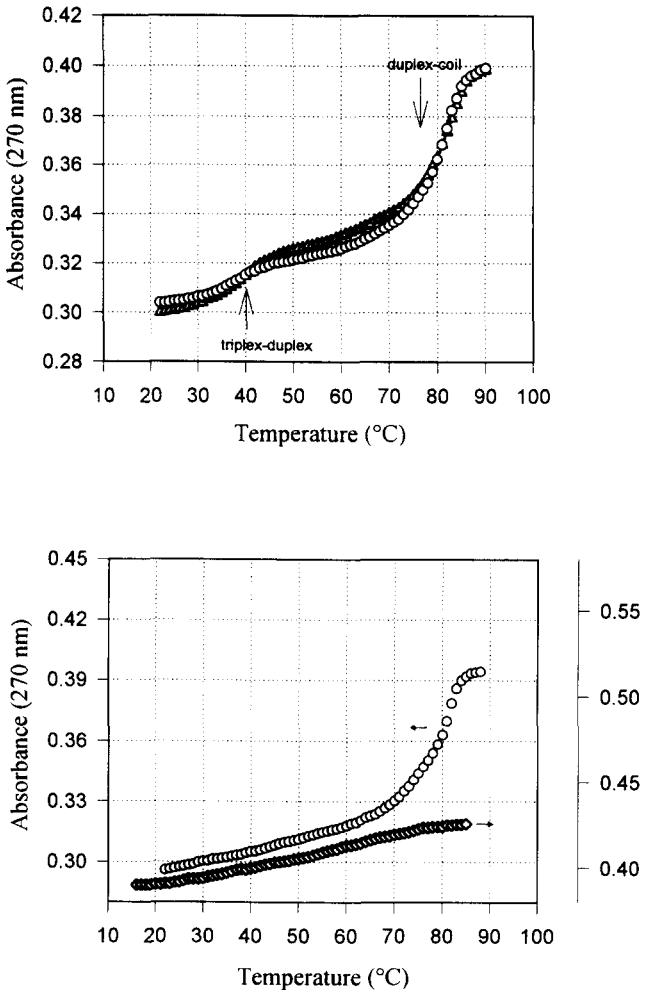

Fig. 4. (Top) UV-absorbance melting profile in standard buffer of the triplex made by the 20GT and 30RY at equimolar ratio. ○ represents the denaturing profile, whereas △ represents the renaturing profile. The experiment was performed using a 0.5 cm quartz cuvette, containing a DNA triplex at a concentration of 0.44 μM and increasing and decreasing the temperature at a rate of 0.5°C/min. (Bottom) UV-absorbance melting profiles of duplex 30RY alone (~0.8 μM) (○) and oligonucleotide 20GT alone (~3 μM) (◇) in standard buffer.

3.4. Ultraviolet spectroscopy

Melting experiments of 1:1 30GT:30RY mixtures have been performed in standard buffer at DNA concentrations between 0.084 and 3.6 μM in triplex (concentrations higher than 3.6 μM induced aggregation of 20GT). Fig. 4 (top) shows typical ascending and discending melting profiles of a solution containing triplex DNA 0.44 μM, obtained following the variation of the UV absorbance at 270 nm, as the temperature was increased and decreased from 20 to 90°C at the rate of 0.5°C/min. Note that the shapes of the melting profiles are biphasic. The high-temperature transition (*transition 2*) is due to the denaturation of the target duplex 30RY, whereas the low-temperature transition (*transition 1*) is due to the duplex-to-triplex transformation. Transition 1 has a transition width δt~18°C, a hyperchromicity ($[A^{50°} - A^{25°}]/A^{50°}$) of ~6% and T_ms varying from 34 (0.084 μM in triplex) to 43°C (3.69 μM in triplex). Moreover, transition 1 can be considered with good approximation to be reversible at a heating/cooling rate of 0.5°C/min. Fig. 4 (bottom) reports the individual melting profiles of 30RY and 20GT, which show that transition 1 is not present in neither of them.

3.5. Thermodynamic analysis

The denaturation of triplex 20GT:30RY can be written as:

$$30\ RY:20GT \overset{K_{HG}}{\rightleftharpoons} 30\ RY + 20GT \overset{K_{WC}}{\rightleftharpoons} coil + 20\ GT \quad (1)$$

where K_{HG} and K_{WC} are equilibrium constants for transitions 1 and 2, respectively. Applying a two-state model to transition 1 one obtains that [5–7, 34]:

$$\frac{1}{T_m} = \frac{-R}{\Delta H_{HG}} \ln C_T + \frac{(\Delta S_{HG} + 0.223R)}{\Delta H_{HG}} \quad (2)$$

where C_T is the total concentration of 20GT in μM strand, ΔH_{HG} and ΔS_{HG} are the enthalpy and entropy changes of triplex dissociation, and R is the gas constant. A plot of $1/T_m$ versus $\ln(C_T)$ gives a straight line whose slope and y-intercept provide the ΔH_{HG} and ΔS_{HG} for triplex dissociation. Fig. 5 (top) shows such a plot for triplex 20GT:30RY, which gives values of ΔH_{HG} = 79 kcal/mol, ΔS_{HG} = 224 cal/K·mol and ΔG_{HG} = 12.2 kcal/mol ($\Delta G = \Delta H$-298ΔS). Fig. 5 also shows a $1/T_m$ versus $\ln(C_T)$ plot for duplex 30RY, from which values of ΔH_{WC} = 169 kcal/mol of duplex, ΔS_{WC} = 449 cal/K·mol of duplex were obtained.

Alternatively, ΔH of triplex formation was evaluated by a shape analysis of UV melting curves according to equation [34]:

$$\Delta H_{HG} = 2(n+1)RT_m^2\left(\frac{\delta\alpha}{dT}\right)_{T_m} \quad (3)$$

where n = 2 (bimolecular process), T_m is the melting temperature of transition 1 and α the fraction of dissociated triplex at a given temperature. Fig. 5 (bottom) shows typical versu T curves obtained from UV-melting curves of solutions at different triplex concentrations. Such analyses gave an average ΔH of 87 kcal/mol, which is in fairly good accord with the ΔH obtained from $1/T_m$ versus $\ln(C_T)$, considering that the error involved in van't Hoff analyses is roughly 10%. It is interesting

Table 1
Thermodynamic parameters for triplex formation in 50 mM Tris-acetate (pH 6 or 7.4), 50 mM NaCl, 10 mM $MgCl_2$

Triplex	ΔH (kcal/mol	ΔS (cal/K·mol)	ΔG (kcal/mol	T_m (°C)	Conc. (μM)	pH
20GT:30RY	79	224	12	39	0.44	7.4
(Y·RY)[a]	86	245	13	43	2.2	6
I (Y·RY)[b]	92	268	12.4	37	1.7	6
II (R·RY)[c]	80	226	13.4	54	–	7.3

Triplex I is formed by duplex d(TGAAAAAGAAAGGAAGAAGAAAGGG)·d(ACTTTTTCTTTCCTTCTTCTTTCCC) and oligonucletide d(CTTTCCTTCTTCTTTCCC), see [13]. [b]Triplex II is formed by duplex d(TGAAAAAGAAAGGAAGAAGAAAGGG)·d(ACTTTTTCTTTCCTTCTTCTTTCCC) and oligonucletide d(TTTccTTcTTcTTTccccT) (c = m^5C) [37]. Triplex III is formed by duplex d(CCCTTTTCCC)d(GGGAAAAGGG) and oligonucletide d(GGGAAAAGGG) [19], buffer is 10 mM cocodylate, pH 7.3, 50 mM $MgCl_2$, 0.1 mM EDTA.

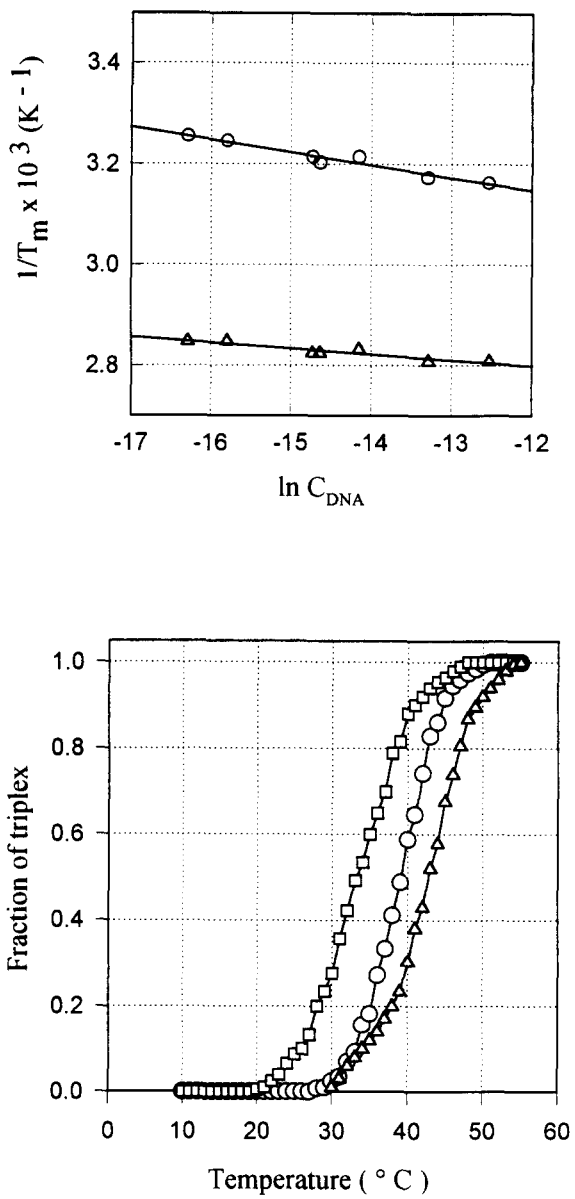

Fig. 5. (Top) Plot of $1/T_m$ versus $\ln(C_T)$ of triplex 20GT:30RY in standard buffer. The DNA concentration varies from 0.084 to 3.62 μM. The plot with symbols ○ was obtained with the T_m values of the triplex/duplex transformation, the plot with symbols △ was obtained with the T_m of the *duplex-coil* transformation. The straight lines represent the linear regression of the experimental points. (Bottom) Fraction of triplex as a function of T obtained from individual melting profiles recorded at different DNA concentration. From the slope of these curves at the semitransition point, the ΔH of triplex formation was evaluated according to equation 3. DNA triplex concentrations are: 0.085 μM (□), 0.44 μM (○), 1.7 μM (△).

to compare the thermodynamic parameters for triplex formation by the G-rich oligonucleotide 20GT and duplex 30RY with the parameters determined for YRY triplexes of comparable size (Table 1). The enthalpy content of triplex 20GT:30RY appears to be somewhat lower than the ΔHs of both Y·RY triplexes (triplex I contains 18 triads [13]; triplex II contains 17 triads; see Table 1). This can be attributed to the fact that the triads of a R·RY triplex, G·GC and T·AT, are not isomorphous, contrarily to C^+·GC and T·AT triads of the Y·RY motif [1]. As revealed by a combined NMR and molecular dynamic study, the third (G,T)-strand in a R·R·Y triplex seems to come up with distortions, which are likely to influence the stacking between adjacent bases [28]. Moreover, another factor that can increase the enthalpy contents of Y·RY triplexes might be the effect of cytosine protonation [5]. As for the entropy contents of 20GT:30RY, this is also lower than the ΔHs of triplexes I and II. Considering the solvation of DNA, the process of triplex formation can be written as:

$$\text{duplex}\cdot nH_2O + \text{oligonucleotide}\cdot mH_2O \rightleftharpoons \text{triplex}\cdot pH_2O + \{(n+m)-p\}H_2O$$

where nH_2O and mH_2O represent the ordered water around the duplex and the oligonucleotide, whereas $\{(n+m)-p\}H_2O$ is the water released when the oligonucleotide and the duplex come together (a source of positive entropy). It is possible that a (G,T)-oligonucleotide promotes a larger release of water molecules than a (C,T)-oligonucleotide does.

Surprisingly, the shorter 10-triad triplex $d(C_3T_4C_3)\cdot d(G_3A_4G_3)\cdot d(G_3A_4G_3)$ ($\Delta G = -13.4$ kcal/mol, T_m~54°C) is much more stable than triplex 20GT:30RY ($\Delta G = -12.2$ kcal/mol, T_m~40°C), but the first system had been studied under very different conditions (50 mM $MgCl_2$, absence of monovalent cations) [19]. It seems that in a R·RY triplex, the A·AT triad is more stabilising than the T·AT one. To gain insight into this property we tried to study the interaction between 30RY and the analog oligonucleotide d(AGGGAGGGAGGAAGGGAGGG), but this sequence, contrarily to 20GT, aggregates quickly in solution.

In conclusion, the data here reported show that in near physiological conditions (50 mM Tris-acetate, pH 7.4, 50 mM NaCl, 10 mM $MgCl_2$, 0.1 mM spermine), the G-rich oligonucleotide 20GT is able to recognise and form a stable triplex ($\Delta G = -12.2$ kcal/mol) with a critical R·Y sequence located in the promoter of the Ki-*ras* proto-oncogene. This finding is useful in designing artificial repressors capable to inhibit, in a sequence-specific manner, the expression of the Ki-*ras* gene which is involved in the genesis of several tumors [35]. We have tested in vitro the ability of 20GT to inhibit the transcription of a recombinant template containing the critical R·Y site of Ki-*ras* and proved that this 20-mer oligonucleotide can act as a repressor, although it exhibited some aggregation under transcription conditions (conc. > 20 μM). In a recent study it has been shown that G-rich oligonucleotide aggregation is favoured by K^+ [36]. Work is in progress in our laboratory in order to test in vivo the capacity of 20GT to inhibit the expression of a recombinant vector containing the CAT gene under the control of the Ki-*ras* promoter.

Acknowledgements: This work has been carried out with the financial support of the Italian Ministry of University and Scientific Research (Murst 60%).

References

[1] Sun, J.-S. and Hélène, C. (1993) Curr. Opin. Struct. Biol. 3, 345–356.
[2] Moser, H.E. and Dervan, P.B. (1987) Science 238, 645–650.
[3] François, J.-C., Saison-Behmaras, T. and Hélène, C. (1988) Nucleic Acids Res. 16, 11431–11440.
[4] Lyamichev, V.L., Mirkin, S.M., Frank-Kamenetski, M.D. and Cantor, C.R. (1988) Nucleic Acids Res. 16, 2165–2178.
[5] Manzini, G., Xodo, L.E., Gasparotto, D., Quadrifoglio, F., van

der Marel, G.A. and van Boom, J.H. (1990) J. Mol. Biol. 213, 833–843.
[6] Xodo, L.E., Manzini, G. and Quadrifoglio, F. (1990) Nucleic Acids Res. 18, 3557–3564.
[7] Xodo, L.E., Manzini, G., Quadrifoglio, F., van der Marel, G.A. and van Boom, J.H. (1991) Nucleic Acids Res. 20, 5625–5631.
[8] Pilch, D.S., Brousseau, R. and Shafer, R.H. (1990) Nucleic Acids Res. 18, 5743–5750.
[9] Roberts, R.W. and Crothers, D.M. (1991) Proc. Natl. Acad. Sci. USA 88, 9397–9401.
10] Plum, G.E., Park, Y.W., Singleton, S.F., Dervan, P.B. and Breslauer, K.J. (1990) Proc. Natl. Acad. Sci. USA 87, 9436–9440.
11] Wilson, W.D., Hopkins, H.P., Mizan, S., Hamilton, D.D. and Zon, G. (1994) J. Am. Chem. Soc. 116, 3607–3608.
12] Volker, J., Botes, D.P., Lindey, G.G. and Klump, H.H. (1993) J. Mol. Biol. 230, 1278–1290.
13] Xodo, L.E. (1995) Eur. J. Biochem 228, 918–926.
14] Rajagopal, P. and Feigon, J. (1989) Nature 339, 637–640.
15] De los Santos, C., Rosen, M. and Patel, D. (1989) Biochemistry 28, 7282–7289.
16] Cooney, M., Czernuszewicz, G., Postel, E.H., Flint, S.J. and Hogan, M. (1988) Science 241, 456–459.
17] Beal, P.A. and Dervan, P.B. (1991) Science 251, 1360–1363.
18] Durland, R.H., Kessler, D.J., Gunnell, S., Duvic, M., Pettitt, B.M. and Hogan M.E. (1991) Biochemistry 30, 9246–9255.
19] Pilch, D.S., Leverson, C. and Shafer, R.H. (1991) Biochemistry 30, 6081–6087.
[20] Marck, C. and Thiele, D. (1978) Nucleic Acids Res. 5, 1017–1028.
[21] Thiele, D., Marck, C., Schneider, C. and Guschlbauer, W. (1978) Nucleic Acids Res. 5, 1997–2012.
[22] Broitman, S.L., Im, D.D. and Fresco, J.R. (1987) Proc. Natl. Acad. Sci. USA 84, 5120–5124.
[23] Kohwi, Y. and Kohwi-Shigematsu, T. (1989) Proc. Natl. Acad. Sci. USA 85, 3781–3785.
[24] McShan, M.W., Rossen, R.D., Laughter, A.H., Trial, J., Kessler, D.J., Zendgui, J.G., Hogan, M.E. and Orson, F.M. (1992) J. Biol. Chem. 267, 5712–5721.
[25] Roy, C.(1993) Nucleic Acids Res. 12, 2845–2852.
[26] Postel, E.H., Flint, S.J., Kessler, D.J. and Hogan, M.E. (1991) Proc. Natl. Acad. Sci. USA 88, 8227–8231.
[27] Mayfield, C., Squibb, M. and Miller, P. (1994) Biochemistry 33, 3358–3363.
[28] Radhakrishnan, I. and Patel, D. (1993) Structure 1, 135–152.
[29] Cheng, A.-J. and Van Dyke, M.W. (1994) Nucleic Acids Res. 22, 4742–4747.
[30] Hoffman, E.K., Trusko, S.P., Murphy, M. and George, D. (1990) Proc. Natl. Acad. Sci. USA 87, 2705–2709.
[31] Bernardi, G. (1971) Methods Enzymol. 21, 95–139.
[32] Fu-Ming Chen (1991) Biochemistry 30, 4472–4479.
[33] Antao, V.P., Gray, D.M. and Ratliff, R.L. (1988) Nucleic Acids. Res. 16, 719–729.
[34] Marky, L. and Breslauer, K. (1987) Biopolymers 26, 1601–1620.
[35] Lowy, D.R. and Willumsen, B.M. (1993) Annu. Rev. Biochem. 62, 851–891.
[36] Olivas, W.M. and Maher, L.J. (1995) Biochemistry 34, 278–284.
[37] Xodo L.E. (1995) unpublished data.